New bent-shaped liquid crystalline derivatives of 2,7-dihydroxynaphthalene containing lateral bromine atoms

N. S. Novikova[a]; E. Gorecka[b]; R. V. Kondratyeva[a]; E. D. Kilimenchuk[a]

[a] Physico-Chemical Institute A.V. Bogatskiy, National Academy of Sciences of Ukraine, Odessa, Ukraine [b] Department of Chemistry, Warsaw University, 02-089 Warsaw, Poland

PLEASE SCROLL DOWN FOR ARTICLE

Taylor & Francis
Taylor & Francis Group

New bent-shaped liquid crystalline derivatives of 2,7-dihydroxynaphthalene containing lateral bromine atoms

N. S. Novikova[a], E. Gorecka[b]*, R. V. Kondratyeva[a] and E. D. Kilimenchuk[a]

[a]*Physico-Chemical Institute A.V. Bogatskiy, National Academy of Sciences of Ukraine, Lustdorfskay doroga, 86, Odessa, 65080, Ukraine;* [b]*Department of Chemistry, Warsaw University, ul. Żwirki I Wigury 101, 02-089 Warsaw, Poland*

New banana-shaped mesogens with a naphthalene central ring were synthesised. The presence of a lateral substituent, i.e. a bromine atom in a phenyl group localised near the central naphthalenic ring, drastically decreases the clearing and melting temperatures of these materials and favours formation of a nematic phase. The smectic phase is observed only for the longest homologues (for $n > 12$). The observed smectic B phase is of the antiferroelectric, synclinic type in a virgin sample, but when relaxed after application of an electric field, an antiferroelectric, anticlinic structure with $45°$ tilt is formed, as suggested by texture with zero birefringence.

Keywords: 2,7-dihydroxynaphtalene esters; banana-shaped mesogens; spontaneous polarisation

1. Introduction

The discovery that molecules with a bent-shaped core (commonly known as 'banana' molecules) form polar smectic phases opened a new field in liquid crystal (LC) research (*1*). In these materials, polarisation, tilt and layer undulations can develop independently; thus bent-core mesogens exhibit a much richer variety of smectic and columnar phases than rod-like molecules. In addition, the switching mechanism in an electric field is more complicated. Dipole moments can adjust their directions to the electric field by two competing mechanisms: rotation around the long molecular axis or rotation on the tilt cone around the layer normal (*2*). A detailed description of liquid crystalline banana phases is provided in the literature (*3–8*). It is worth noting that about four years ago the nomenclature of banana phases underwent significant changes, as reflected in the review by Tschierske and Dantlgraber (*9*).

One of the main goals in LC research is to find the relationship between a chemical structure and the type of mesophase (*10–12*). It has been found that the main molecular factors determining the type of mesomorphism are bend angle between molecular branches, number of aromatic cycles in molecular branches as well as the nature and the direction of the linking groups in the branches. In some materials also the size, electronic nature and position of the lateral substituents connected either to the central fragment or to the branches are very important. In our work, we focused on 2,7-dihydroxynaphtalene derivatives; we anticipated that a large and flat central fragment of the molecules should encourage formation of banana phases with strongly hindered rotation of molecules, which should result in high values of the electric spontaneous polarisation of these materials. There have been several attempts to obtain naphthalene-based banana molecules before, but since most of these materials have very high melting and clearing temperature (usually above $200°C$) at which decomposition is often observed, only few systematic studies have been performed. Banana-shaped 2,7-dihydroxynaphthalene derivatives containing a pyrimidine cycle in their branch fragments have been described (*13*). If in 2,7- dihydroxynaphthalene esters an azomethine bond is used as the second linking group then the compounds exhibit smectic phases (*14*). Introduction of a Cl atom or CH_3 group at the 1-position of a naphthalenic cycle led to formation of B_2 phases, whereas introduction of a CN group led to nematic (N) phases and a phase transition between chiral and racemic B_2 phases (*15*). Replacement of the azomethine linking groups by esters generally favours formation of B_1 phases, although with an increase of the terminal alkoxy chain length for derivatives with lateral Cl and CH_3 groups a B_2 phase was observed and for CN and NO_2 derivatives a B_7 phase was observed (*16*). In addition, the influence of the lateral substituent in molecular branches has been studied by Amaranata Reddy and Sadashiva (*17*). In a subsequent paper, asymmetrical 2,7-dihydroxynaphthalene derivatives containing a fluorine atom only in one of the lateral branches were described (*18*). The shorter homologues of the fluorinated compounds form two modifications of the liquid crystal phase: B_1 and N, the longer homologues form only lamellar B_2 phase.

In this work we focused on the influence of the lateral substituent, i.e. a bromine atom placed on one of the phenyl rings in the molecular branch. It was found that such a lateral substituent significantly decreases the clearing and melting temperatures and favours a nematic phase.

2. Experimental

Physical investigations

^{1}H NMR spectra of 5–10% solutions of the studied compounds were recorded using a Varian VXR-300 spectrometer with an operating frequency of 300 MHz. Mass spectra were investigated using a MX-1321 spectrometer with a direct application system with an input electron ionizing energy of 70 eV and the ionisation chamber at 220°C, and also using a VG 70-70EQ mass spectrometer in FAB mode by use of a bunch of Xe atoms with an energy of 8 kV and 3-nitrobenzilic alcohol and polypropylene glycol as a matrix. IR spectra were recorded in CHCl$_3$ solution with a Specord IR-75 spectrophotometer. Temperatures of the phase transitions were studied by polarising optical microscopy (POM) using POLAM P-312 and differential scanning calorimetry (Perkin Elmer DSC7). For X-ray studies, the Bruker Nanostar system was used with a two-dimensional (2D) positional sensitive area detector that allows signals corresponding to the periodicities in the range 18–500 Å to be observed. High-angle reflections (periodicities in the range 2–40 Å) were measured using a Bruker D8 Discover system. Spontaneous polarisation was detected by a peak current method using 5 μm thick cells with ITO transparent electrodes. The same type of cell was also used for observation of the sample texture in an electric field. Molecular dimensions were simulated using the HyperChem package.

Synthesis

In the first stage of the synthesis (Scheme 1), the key intermediates, 4-(4-*n*-alkoxybenzoyloxy)-3-bromobenzoic acids were prepared, and then esterification of 2,7-dihydroxynaphthalene by carbodiimide was carried out. 3-Bromo-4-hydroxybenzoic acid (**2**) was obtained by the known method (*19*). 4-Alkoxybenzoyl chlorides (**4a–4f**) were prepared by interaction of 4-alkoxybenzoic acids with thionyl chloride (*20*). The 4-(4-*n*-alkoxybenzoyloxy)-3-bromobenzoic acids (**5a–5f**) were obtained from compound **2** by acylation of 4-*n*-alkoxybenzoyl chlorides (**4a–4f**) in dry pyridine. In the next step, 4-(4-*n*-alkoxybenzoyloxy)-3-bromobenzoic acids (**5a–5f**) are

obtained. The purity of the acids was confirmed using thin-layer chromatography (TLC) and the molecular structure was proved via NMR data.

Etherification of 2,7-dihydroxynaphthalene by ester acids was carried out by a carbodiimidic method with addition of 4-dimethylaminopyridine in the environment of dry chloroform. Final products were purified by column chromatography and a few crystallisations. The purity of 2,7-bis[4-(4-*n*-alkoxybenzoyloxy)-3-bromobenzoyloxy]naphthalenes (**7a–7f**) was confirmed by TLC, and their molecular structure confirmed via NMR spectra.
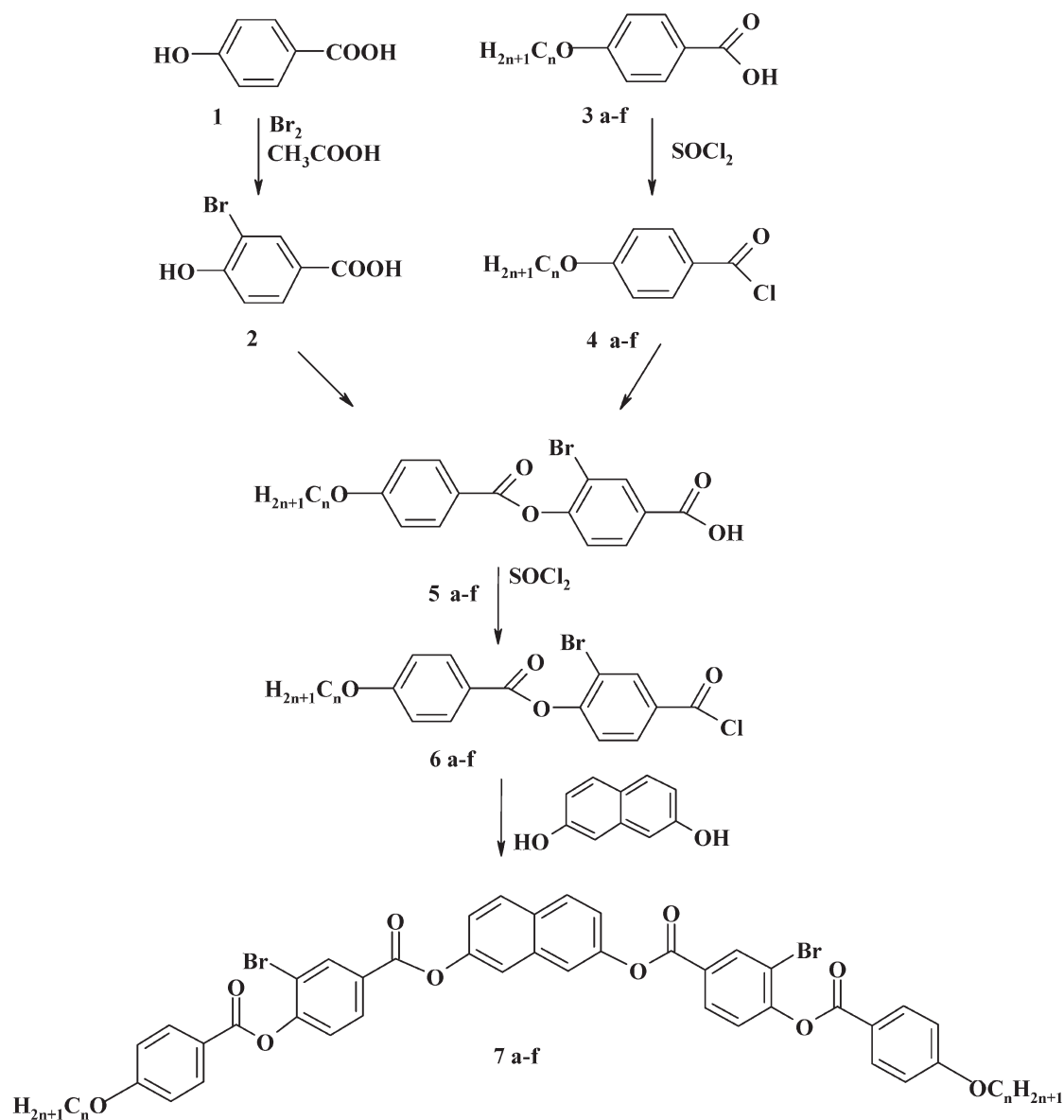
4-(4-n-Alkoxybenzoyloxy)-3-bromobenzoic acids (5a–5f).

To a suspension of 3-bromo-4-hydroxybenzoic acid (0.024 mol) in dry pyridine (30 ml) the corresponding 4-alkoxybenzoyl chloride (0.024 mol) was added dropwise and stirred at 20°C for 21 h. The reaction mixture was poured into ice water (100 ml), which was acidified by hydrochloric acid up to pH=2. The resulting white precipitate was filtered, washed with water up to pH=7.0, dried, suspended in cold alcohol (~300 ml) and filtered again. The deposited crude product was crystallised from benzene. The phase transition temperatures of compounds **5a–5f** are presented in Table 1.

For 4-(4-*n*-heptyloxybenzoyloxy)-3-bromobenzoic acid (**5a**), yield 46%. ^{1}H NMR (300 MHz, CDCl$_3$): δ 8.42 (d, 1H, ArBr), 8.20 (d, 2H, Ar), 8.14–8.12 (d.d, ^3J=8.40 Hz, ^4J=1.86 Hz, 1H, ArBr), 7.43 (d, ^3J=8.41 Hz, 1H, ArBr), 7.00 (d, ^3J=9.02 Hz, 2H, Ar), 4.06 (t, J=6.53 Hz, 2H, OCH$_2$), 1.89–1.77 (m, 2H, OCH$_2$CH$_2$), 1.56–1.41 (m, 2H, CH$_2$), 1.40–1.15 (m, 6H, CH$_2$), 0.88 (t, J=6.53 Hz, 3H, CH$_3$). Elemental analysis: C$_{21}$H$_{23}$BrO$_5$ requires C 57.23, H 5.29, Br 18.39; found C 57.93, H 5.29, Br 18.2%.

For 4-(4-*n*-octyloxybenzoyloxy)-3-bromobenzoic acid (**5b**), yield 77.3%. ^{1}H NMR (300 MHz, CDCl$_3$): 8.42 (d, ^4J=2.18 Hz, 1H, ArBr), 8.20 (d, ^3J=9.02 Hz, 2H, Ar), 8.13–8.11 (d.d, ^3J=8.41 Hz, ^4J=1.87 Hz 1H, ArBr), 7.43 (d, ^3J=8.41 Hz, 1H, ArBr), 7.00 (d, ^3J=9.02 Hz, 2H, Ar), 4.06 (t, J=6.54 Hz, 2H, OCH$_2$), 1.89–1.75 (m, 2H, OCH$_2$CH$_2$), 1.75–1.55 (m 2H, CH$_2$), 1.40–1.16 (m, 8H, CH$_2$), 0.89 (t, J=6.54 Hz, 3H, CH$_3$). Elemental analysis: C$_{22}$H$_{25}$BrO$_5$ requires C 58.79, H 5.57, Br 17.82; found C 58.63, H 5.72, Br 17.73%.

For 4-(4-*n*-nonyloxybenzoyloxy)-3-bromobenzoic acid (**5c**), yield 64%. ^{1}H NMR (300 MHz, CDCl$_3$): 8.42 (d, ^4J=2.18 Hz, 1H, ArBr), 8.20 (d, ^3J=9.02 Hz, 2H, Ar), 8.14–8.12 (d.d, ^3J=8.40 Hz, ^4J=1.86 Hz 1H, ArBr), 7.43 (d, ^3J=8.40 Hz, 1H, ArBr), 6.99 (d, ^3J=9.02 Hz, 2H, Ar), 4.06 (t, J=6.53 Hz, 2H, OCH$_2$),

Scheme 1. Synthesis of target compounds **7a–7f**.

1.89–1.77 (m, 2H, OCH$_2$<u>CH$_2$</u>), 1.55–1.41 (m, 2H, CH$_2$), 1.41–1.19 (m, 10H, CH$_2$), 0.89 (t, J=6.53 Hz, 3H, CH$_3$). Elemental analysis: C$_{23}$H$_{27}$BrO$_5$ requires C 59.61, H 5.83, Br 17.28; found C 59.88, H 5.97, Br 17.49%.

For 4-(4-*n*-decyloxybenzoyloxy)-3-bromobenzoic acid (**5d**), yield 46%. ^{1}H NMR (300 MHz, CDCl$_3$): δ 8.42 (d, ^4J=2.18 Hz, 1H, ArBr), 8.20 (d, ^3J=9.02 Hz, 2H, Ar), 8.13–8.11 (d.d, ^3J=8.40 Hz, ^4J=1.80 Hz, 1H, ArBr), 7.43 (d, ^3J=8.40 Hz, 1H, ArBr), 6.99 (d,

Table 1. Phase transition temperatures (°C) of 4-(4-*n*-alkoxybenzoyloxy)-3-bromobenzoic acids (**5a–5f**).

Compound	n	Cr		Sm		N		I
5a	7	•	121.0	–		•	186.0	•
5b	8	•	111.0	–		•	173.0	•
5c	9	•	144.0	–		•	183.0	•
5d	10	•	117.0	–		•	187.0	•
5e	12	•	129.3	–		•	176.4	•
5f	16	•	104.0	•	147	•	167.0	•

^3J=9.03 Hz, 2H, Ar), 4.06 (t, J=6.53 Hz, 2H, CH$_2$O), 1.89–1.76 (m, 2H, OCH$_2$C$\underline{H_2}$), 1.55–1.41 (m, 2H, CH$_2$), 1.41–1.15 (m, 12H, C$\underline{H_2}$), 0.89 (t, J=6.53 Hz, 3H, CH$_3$). Elemental analysis: C$_{24}$H$_{29}$BrO$_5$ requires C 60.38, H 6.08, Br 16.77; found C 60.6, H 6.25, Br 16.61%.

For 4-(4-*n*-dodecyloxybenzoyloxy)-3-bromobenzoic acid (**5e**), yield 75%. ^{1}H NMR (300 MHz, CDCl$_3$): δ 8.42 (d, ^4J=2.18 Hz, 1H, ArBr), 8.20 (d, ^3J=8.71 Hz, 2H, Ar), 8.13–8,11 (d.d, ^3J=8.41 Hz, ^4J=1.87 Hz, 1H, ArBr), 7.43 (d, ^3J=8.40 Hz, 1H, ArBr), 6.99 (d, ^3J=9.01 Hz, 2H, Ar), 4.06 (t, J=6.54 Hz, 2H, OCH$_2$), 1.89–1.76 (m, 2H, OCH$_2$C$\underline{H_2}$), 1.55–1.41 (m, 2H, CH$_2$), 1.41–1.15 (m, 16H, C$\underline{H_2}$), 0.89 (t, J=6.54 Hz, 3H, CH$_3$). Elemental analysis: C$_{26}$H$_{33}$BrO$_5$ requires C 61.78, H 6.53, Br 15.84; found C 61.93, H 6.75, Br 15.68%.

For 4-(4-*n*-hexadecyloxybenzoyloxy)-3-bromobenzoic acid (**5f**), yield 73.0%. ^{1}H NMR (300 MHz, CDCl$_3$): δ 8.42 (d, ^4J=2.18 Hz, 1H, ArBr), 8.19 (d, ^3J=8.71 Hz, 2H, Ar), 8.13–8.11 (d.d, ^3J=8.41 Hz, ^4J=1.86 Hz, 1H, ArBr), 7.42 (d, ^3J=8.41 Hz, 1H, ArBr), 7.00 (d, ^3J=9.02 Hz, 2H, Ar), 4.06 (t, J=6.54 Hz, 2H, OCH$_2$), 1.92–1.74 (m, 2H, OCH$_2$C$\underline{H_2}$), 1.56–1.42 (m, 2H, CH$_2$), 1.41–1.18 (m, 24H, C$\underline{H_2}$), 0.88 (t, J=6.54 Hz, 3H, CH$_3$). Elemental analysis: C$_{30}$H$_{41}$BrO$_5$ requires C 64.12, H 7.3, Br 14.26; found C 64.33, H 7.57, Br 14.16%.

4-(4-n-Alkoxybenzoyloxy)-3-bromobenzoyl chlorides

4-(4-*n*-Alkoxybenzoyloxy)-3-bromobenzoyl chlorides were prepared by interaction 4-(4-*n*-alkoxybenzoyloxy)-3-bromobenzoic acids (0.0074 mol) with thionyl chloride (0.0148 mol) in dry benzene (30 ml) while stirring and cooling down to 10°C for about 30 min. Next the reaction mixture was boiled for 9 h on a water bath. Benzene and thionyl chloride were removed at lowered pressure, dry benzene (15 ml) was added to the remainder and benzene was removed again. 4-(4-*n*-Alkoxybenzoyloxy)-3-bromobenzoyl chlorides were used in following synthesis without additional purification.

2,7-Bis[4-(4-n-alkoxybenzoyloxy)-3-bromobenzoyloxy]naphthalenes (7a–7f)

A mixture of 4-(4-*n*-alkoxybenzoyloxy)-3-bromobenzoic acids (0.01 mol), 4-dimethylaminopyridine (0.2 g, 0.001 mol) and 2,7-dihydroxynaphtalene (0.005 mol) in dry chloroform (25 ml) was stirred for 10 min. Then *N,N*-dicyclohexylcarbodiimide (0.06 mol) was added and the reaction mixture was stirred at a room temperature for 16 h. The reaction was controlled using a TLC method on Sorbfil plates. The crude was filtered off and the filtrate diluted with chloroform (100 ml), washed by 5% solution of acetic acid (2 × 50 ml), then by 5% aqueous solution of NaOH (2 × 25 ml) and water (3 × 25 ml) up to pH=7. The solution was dried using magnesium sulfate. Chloroform was removed away at lowered pressure. The precipitate was crystallised from a mixture of acetonitrile/chloroform (3:2) and then purified by column chromatography with chloroform eluent. After removing of the eluent the remainder was crystallised twice from a acetonitrile/chloroform (3:2) mixture. The phase transition temperatures of compounds **7a**–**7f** are presented in Table 2.

For 2,7-bis-[4-(4-*n*-heptloxybenzoyloxy)-3-bromobenzoyloxy]naphthalene (**7a**), MS m/z: 1028 [M+]. ^{1}H NMR (300 MHz, CDCl$_3$): δ 8.55 (d, ^4J=2.18 Hz, 2H, ArBr), 8.29–8.26 (d.d, ^3J=8.71 Hz, ^4J=1.87 Hz, 2H, ArBr), 8.21 (d, ^3J=8.72 Hz, 4H, Ar), 7.97 (d, ^3J=9.03 Hz, 2H, naphthyl), 7.71 (d, ^4J=2.18 Hz, 2H, naphthyl), 7.48 (d, ^3J=9.03 Hz, 2H, ArBr), 7.4–7.37 (d.d, ^3J=8.71 Hz, ^4J=2.17 Hz, 2H, naphthyl), 7.02 (d, ^3J=9.03 Hz, 4H, Ar), 4.07 (t, J=6.53 Hz, 4H, OCH$_2$), 1.91–1.77 (m, 4H, C$\underline{H_2}$CH$_2$O), 1.61–1.22 (m, 16H, CH$_2$), 0.91 (t, J=6.53 Hz, 3H, CH$_3$). Elemental analysis: C$_{52}$H$_{50}$Br$_2$O$_5$ requires C 62.77, H 5.03, Br 16.1; found C 62.94, H 5.23, Br 16.27%.

For 2,7-bis[4-(4-*n*-octyloxybenzoyloxy)-3-bromobenzoyloxy]naphthalene (**7b**), MS m/z: 1052 [M+1]. ^{1}H NMR (300 MHz, CDCl$_3$): δ 8.55 (d, ^4J=2.18 Hz, 2H, ArBr), 8.29–8.26 (d.d, ^3J=8.71 Hz, ^4J=1.87 Hz, 2H, ArBr), 8.21 (d, ^3J=8.71 Hz, 4H, Ar), 7.97 (d,

Table 2. Phase transition temperatures (°C) and enthalpies (J g^{-1}, in parentheses) of 2,7-bis[4-(4-*n*-alkoxybenzoyloxy)-3-bromobenzoyloxy]naphthalenes (**7a–7f**).

Comp.	*n*	Cr		B		N		I
7a	7	•	107.3 (66.5)	–		[•]	104.2 (0.4)	•
7b	8	•	94.5 (42.1)	–		[•]	95.4 (0.3)	•
7c	9	•	76.9 (38.2)	–		•	80.04 (0.2)	•
7d*	10	•	68.3 (19.9)	–		•	81.2 (8.9)	•
7e	12	•	60.9 (3.0)	•	79.8 (9.3)	•	84.8 (0.6)	•
7f	16	•	99.7 (8.4)	[•]		–	98.7 (10.9)	•

Cr=crystal; N=nematic phase; B="banana" mesophase; I - isotropic liquid; [ ] indicates monotropic phase. Since all materials have rich crystal polymorphism as a melting temperature of the material the melting of the most stable crystal form is given.

$^3J=9.03$ Hz, 2H, naphthyl), 7.71 (d, $^4J=2.18$ Hz, 2H, naphthyl), 7.48 (d, $^3J=9.03$ Hz, 2H, ArBr), 7.4–7.37 (d.d, 8.71 Hz, $^4J=2.18$ Hz, 2H, naphthyl), 7.02 (d, $J=8.71$ Hz, 4H, Ar), 4.06 (t, $J=6.54$ Hz, 4H, OCH$_2$), 1.89–1.77 (m, 4H, CH$_2$CH$_2$O), 1.59–1.23 (m, 20H, CH$_2$), 0.91 (t, $J=6.54$ Hz, 3H, CH$_3$). Elemental analysis: C$_{54}$H$_{54}$Br$_2$O$_5$ requires C 63.4, H 5.28, Br 15.65; found C 63.68, H 5.43, Br 15.38%.

For 2,7-bis[4-(4-*n*-nonyloxybenzoyloxy)-3-bromobenzoyloxy]naphthalene (**7c**), IR (*v* CHCl$_3$, cm^{-1}): 1710 (C=0), 1595 (arom), 1250 (C–O–C). ^{1}H NMR (300 MHz, CDCl$_3$): δ 8.55 (d, $^4J=2.18$ Hz, 2H, ArBr), 8.29–8.26 (d.d, $^3J=8.71$ Hz, $^4J=2.18$ Hz, 2H, ArBr), 8.21 (d, $^3J=8.71$ Hz, 4H, Ar), 7.97 (d, $^3J=8.72$ Hz, 2H, naphthyl), 7.71 (d, $^4J=2.18$ Hz, 2H, naphthyl), 7.48 (d, $^3J=8.71$ Hz, 2H, ArBr), 7.4–7.37 (d.d, $^3J=8.71$ Hz, $^4J=2.18$ Hz, 2H, naphthyl), 7.02 (d, $^3J=8.72$ Hz, 4H, Ar), 4.06 (t, $J=6.54$ Hz, 4H, OCH$_2$), 1.89–1.77 (m, 4H, CH$_2$CH$_2$O), 1.59–1.23 (m, 24H, CH$_2$), 0.91 (t, $J=6.54$ Hz, 3H, CH$_3$). Elemental analysis: C$_{56}$H$_{58}$Br$_2$O$_5$ requires C 64.0, H 5.52, Br 15.24; found C 64.32, H 5.68, Br 15.47%.

For 2,7-bis-(4-(4-*n*-decyloxybenzoyloxy)-3-bromo-benzoyloxy]naphthalene (**7d**), ^{1}H NMR (300 MHz, CDCl$_3$): δ 8.55 (d, $^4J=2.18$ Hz, 2H, ArBr), 8.28–8.25 (d.d, $^3J=8.71$ Hz, $^4J=2.18$ Hz, 2H, ArBr), 8.21 (d, $^3J=8.71$ Hz, 4H, Ar), 7.97 (d, $^3J=8.71$ Hz, 2H, naphthyl), 7.71 (d, $^4J=2.18$ Hz, 2H, naphthyl), 7.47 (d, $^3J=8.71$ Hz, 2H, ArBr), 7.4–7.37 (d.d, $^3J=8.71$ Hz, $^4J=2.18$ Hz, 2H, naphthyl), 7.01 (d, $^3J=8.71$ Hz, 4H, Ar), 4.06 (t, $J=6.53$ Hz, 4H, OCH$_2$), 1.89–1.77 (m, 4H, CH$_2$CH$_2$O), 1.59–1.23 (m, 28H, CH$_2$), 0.89 (t, $J=6.53$ Hz, 3H, CH$_3$). Elemental analysis: C$_{58}$H$_{62}$Br$_2$O$_5$ requires C 64.56, H 5.75, Br 14.84; found C 64.31, H 5.98, Br 14.84%.

For 2,7-bis[4-(4-*n*-dodecyloxybenzoyloxy)-3-bromobenzoyloxy]naphthalene (**7e**), ^{1}H NMR (300 MHz, CDCl$_3$): δ 8.56 (d, $^4J=2.18$ Hz, 2H, ArBr), 8.28–8.26 (d.d, $^3J=8.71$ Hz, $^4J=2.18$ Hz, 2H, ArBr), 8.21 (d, $^3J=9.03$ Hz, 4H, Ar), 7.97 (d, $^3J=8.72$ Hz, 2H, naphthyl), 7.71 (d, $^4J=2.18$ Hz, 2H, naphthyl), 7.49 (d, $^3J=8.71$ Hz, 2H, ArBr), 7.4–7.37 (d.d, $^3J=8.71$ Hz, $^4J=2.18$ Hz, 2H, naphthyl), 7.02 (d, $^3J=8.71$ Hz, 4H, Ar), 4.06 (t, $J=6.54$ Hz, 4H, OCH$_2$), 1.89–1.77 (m, 4H, CH$_2$CH$_2$O), 1.59–1.21 (m, 36H, CH$_2$), 0.89 (t, $J=6.54$ Hz, 3H, CH$_3$). Elemental analysis: C$_{62}$H$_{70}$Br$_2$O$_5$ requires C 65.60, H 6.17, Br 14.11; found C 65.79, H 6.40, Br 14.41%.

For 2,7-bis[4-(4-*n*-hexadecyloxybenzoyloxy)-3-bromobenzoyloxy]naphthalene (**7f**), IR (*v* CHCl$_3$, cm^{-1}): 1720 (C=O), 1260 (C–O–C). ^{1}H NMR (300 MHz, CDCl$_3$): δ 8.55 (d, $^4J=2.18$ Hz, 2H, ArBr), 8.29–8.26 (d.d, $^3J=8.71$ Hz, $^4J=2.18$ Hz, 2H, ArBr), 8.21 (d, $^3J=9.03$ Hz, 4H, Ar), 7.96 (d, $^3J=8.71$ Hz, 2H, naphthyl), 7.71 (d, $^4J=2.17$ Hz, 2H, naphthyl), 7.48 (d, $^3J=8.72$ Hz, 2H, ArBr), 7.4–7.37 (d.d, $^3J=8.72$ Hz, $^4J=2.18$ Hz, 2H naphthyl), 7.02 (d, $^3J=8.72$ Hz, 4H, Ar), 4.06 (t, $J=6.54$ Hz, 4H, OCH$_2$), 1.89–1.77 (m, 4H, CH$_2$CH$_2$O), 1.57–1.21 (m, 52H, CH$_2$), 0.88 (t, $J=6.54$ Hz, 3H, CH$_3$). Elemental analysis: C$_{70}$H$_{86}$Br$_2$O$_{10}$ requires C 67.41, H 6.90, Br 12.84; found C 67.23, H 6.68, Br 12.6%.

3. Results and discussion

All the synthesised acids **5a**–**5f** are mesomorphic; they form a nematic phases and, moreover, for the longest studied homologue, $n=16$ (**5f**), a smectic phase is also observed. The mesomorphic properties of the rod-like compounds **5a**–**5f** and their phase transition temperatures are sumarised in Table 1.

Comparing the mesomorphic properties of 4-(4-*n*-alkoxybenzoyloxy)-3-bromobenzoic acids and their unsubstituted analogues (*21*) it should be noted that introduction of a bromine atom as a bulky lateral substituent leads to a decrease of the clearing temperature and less complex polymorphism. Homologues **5a**–**5e** with $n=7$–12 carbon atoms, respectively, form only a nematic phase, whereas unsubstituted analogues exhibit two smectic modifications (*19*). In addition, bromine-substituted analogues have a broader mesogenic temperature range and they are easier to purify as starting reagents for synthesis of banana molecules. The transition temperature and mesomorphic properties for these compounds are collected in Table 2.

POM studies clearly revealed that the banana-shaped compounds **7a**–**7f** are mesomorphic. Shorter homologues exhibit only a nematic phase, which is unixaial. The homologue containing 12 carbon atoms in its terminal chain, i.e. material **7e**, exhibits nematic and smectic phases and material **7f** with $n=16$ exhibits only a smectic phase. Both materials **7e** and **7f** in the smectic phase, when observed between glass plates, exhibit fan texture. Between crossed polarisers, optical extinction directions are inclined from polariser directions (Figure 1(a)), which indicates the synclinic tilted structure of the phase with a tilt angle about 40–45°. It should be noted that no stripes are observed, which are characteristic of B$_2$ synclinic-antiferroelectric phases in the presence of chiral domains.

X-ray studies show only single Bragg reflection in the low-angle region. This excludes 2D density modulated structures (like B$_1$-type columnar phases or the B$_7$ phase) and confirms a simple lamellar structure. Moreover, the X-ray measurements confirmed the high tilt of the molecules. For $n=16$ (**7f**) and $n=12$ (**7e**), the Bragg signal corresponds to a
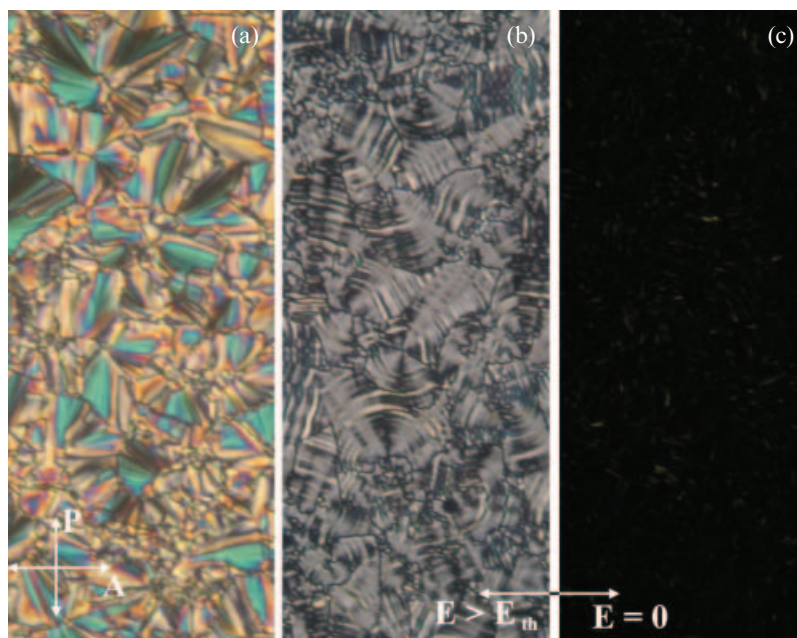
Figure 1. Texture changes in an electric field for material **7f**: (a) sample quickly cooled from an isotropic liquid; (b) the electric field is applied to the sample; (c) the electric field is switched off. Sample thickness was ~5 μm.

layer spacing of ~39.5 Å and 34 Å, respectively, much shorter than the molecular length calculated for the most stretched conformation (see inset of Figure 2).

Applying an electric field causes a sudden and irreversible change of the fan texture. Under electric field, the birefringence of the sample suddenly decreases and fine stripes on the fans are formed (Figure 1 (b)). The extinction direction in the neighbouring stripes alternates. Although it is not possible to determine the angle of extinction precisely since
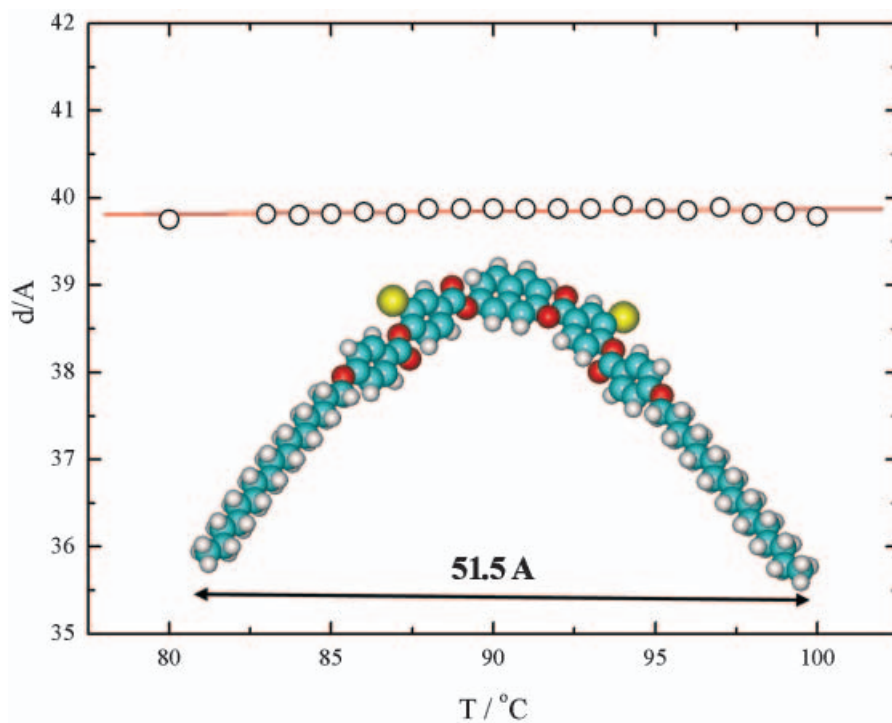

Figure 2. Layer spacing *vs.* temperature for material **7f** in B phase. The molecular structure with indicated molecular length is also shown.

the pattern is too fine, optical tilt for this pattern is in the range $10-20°$. The lower birefringence and lower tilt indicate that the interlayer structure in this state is intermediate between synclinic and anticlinic. Turning off the electric field decreases the birefringence of the sample to nearly zero (Figure 1 C). The zero birefringence in the off-field state suggests anticlinic tilts in consecutive layers with the orthoconic condition fulfilled, i.e. the tilt angle is close to $45°$ (*22*). In consecutive turn on–turn off sequences of the electric field, low birefringence stripe pattern–zero birefringence changes are observed.

The optical changes in an electric field are accompanied by a double current peak (Figure 3). The electric spontaneous polarisation calculated by integration of the peaks area is $250-300 \, nC \, cm^{-2}$, rather typical value for polar phases made of banana molecules.

The behaviour of materials **7e**–**7f** in an electric field is rather unusual. Due to the smallest steric constraints, the molecules in the simple lamellar structure usually adjust their dipole moments to an electric field by collective rotation on the tilt cone. Thus the synclinic antiferroelectric structure, observed for the virgin sample, should convert into the anticlinic ferrroelectric structure in an electric field. When the field is turn off, the sample should relax to synclinic antiferroelectric structure. This is obviously not the case for the studied materials. The synclinic structure under an electric field transforms into a structure intermediate between anticlinic and synclinic and relaxes to anticlinic phase. Apparently this must involve, in some layers, rotation of molecules not only around the cone but also around their long axis (*2*).

Compound **7e** forms a nematic phase above the lamellar B phase. X-ray measurement in temperature range of nematic phase show cybotactic order, which is typical for compounds showing the transition to tilted synclinic smectic phase at lower temperatures. There is no evidence that the nematic phase might be biaxial.

4. Conclusion

In summary, the synthesis of symmetrical 2,7-dihydroxynaphthalene esters containing a bromine atom in the lateral branches has been carried out. Introduction of a bromine atom into the lateral molecular fragment leads to a decrease of phase transition temperature and formation of a nematic phase (compounds **7a**–**7d** with $n=7-10$ carbon atoms). In comparison, the unsubstituted analogues (*17*) form a B_1 phase (homologues with alkyl chain length $n=7$, 8 carbon atoms) and B_2 phase (homologues with longer chain length, $n \geqslant 9$ carbon atoms). Compound **7e** ($n=10$ carbon atoms) shows dimorphism, a nematic phase and a smectic B phase. Further elongation of the alkyl chain length (compound **7f**) leads to disappearance of the nematic phase and only the smectic phase is observed. The observed smectic B phase is of the antiferroelectric, synclinic type in a virgin sample. In a sample exposed to an electric field, in the zero-field state an antiferroelectric, anticlinic
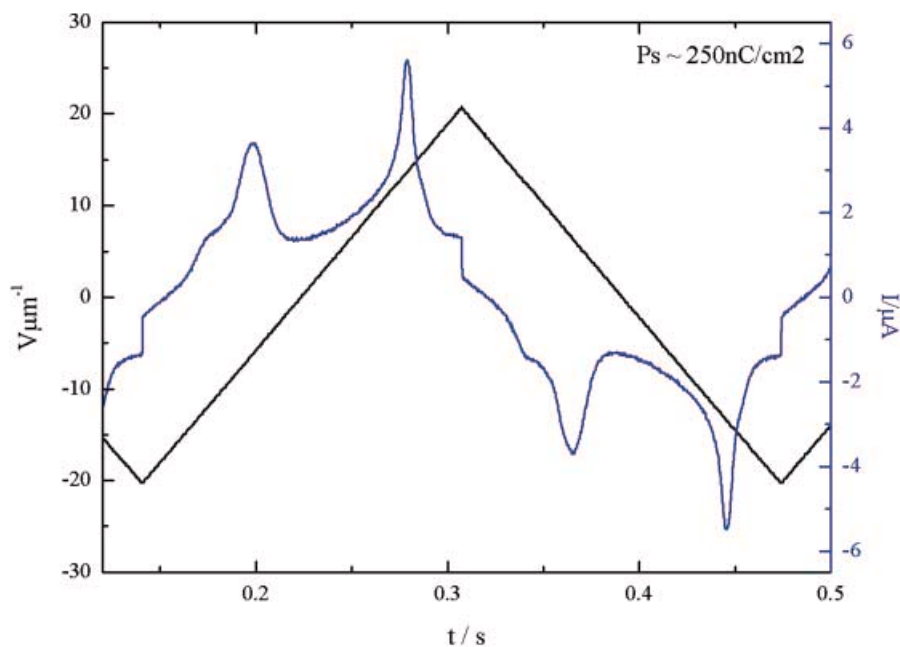

Figure 3. Switching current response observed for material **7f** at $T=90°C$ measured with triangle waveform.

structure with 45° tilt is formed, which is characterised by nearly zero birefringence.

References

(1) Niori T.; Watanabe F.J.; Furukawa T.; Takezoe H. *J. Mater. Chem.* **1996**, *6*, 1231–1233.

(2) Gorecka E.; Vaupotic N.; Pociecha D.; Cepic M.; Mieczkowski J. *ChemPhysChem* **2005**, *6*, 1087–1093.

(3) Brand H.R.; Cladis P.E.; Pleiner H. *Eur. Phys. J. B* **1998**, *6*, 347–353.

(4) Cladis P.E.; Brand H.R.; Pleiner H. *Liq. Cryst. Today* **1999**, *9*, 1–6.

(5) Schmalfuss H.; Shen D.; Tschierske C.; Kresse H. *Liq. Cryst.* **2000**, *27*, 1235–1238.

(6) Schmalfuss H.; Shen D.; Tschierske C.; Kresse H. *Liq. Cryst.* **1999**, *26*, 1767.

(7) Weissflog W.; Kovalenko L.; Wirth J.; Diele S.; Pelzl G.; Schmalfuss H.; Kresse H. *Liq. Cryst.* **2000**, *27*, 677–681.

(8) Macdonald R.; Kentischer F.; Warnick P.; Heppke G. *Phys. Rev. Lett.* **1998**, *81*, 4408–4411.

(9) Tschierske C.; Dantlgraber G. *Pramana J. Phys.* **2003**, *61*, 455–481.

(10) Pelzl G.; Diele S.; Weissflog W. *Adv. Mater.* **1999**, *11*, 707–724.

(11) Thisayukta J.; Nakayama Y.; Watanabe J. *Liq. Cryst.* **2000**, *27*, 1129–1135.

(12) Mieczkowski J.; Matraszek J. *Pol. J. Chem.* **2005**, *79*, 179–209.

(13) Shen D.; Diele S.; Pelzl G.; Wirth I.; Tschierske C. *J. Mater. Chem.* **1999**, *9*, 661–672.

(14) Thisayukta J.; Nakayama Y.; Kawauchi S.; Takezoe H.; Watanabe J. *J. Am. Chem. Soc.* **2000**, *122*, 7441–7448.

(15) Svoboda J.; Novotná V.; Kozmík V.; Glogarová M.; Weissflog W.; Diele S.; Pelzl G. *J. Mater. Chem.* **2003**, *13*, 2104–2110.

(16) Kozmík V.; Kuchař M.; Svoboda J.; Novotná V.; Glogarová M.; Baumeister U.; Diele S.; Pelzl G. *Liq. Cryst.* **2005**, *32*, 1151–1160.

(17) Amaranata Reddy R.; Sadashiva B.K. *Liq. Cryst.* **2000**, *27*, 1613–1623.

(18) Shreenivasa Murthy H.N.; Sadashiva B.K. *Liq. Cryst.* **2004**, *31*, 1347–1356.

(19) Gray G.W.; Brynmor J. *J. Chem. Soc.* **1954**, 2556–2562.

(20) Veygand-Khilgetag M. *Chemistry* **1968**, 234–235.

(21) Kizner T.A.; Mikhaleva M.A.; Serebryakova E.S. *Khim. heterocyclicheskih soedineniy* **1991**, 386–388.

(22) Dhave K. *Ferroelectrics* **2000**, *244*, 415–428.